A COMPARISON OF THE 3D REAL AND COMPLEX VARIABLE BOUNDARY ELEMENT METHODS (BEM)

T.V. HROMADKA II[1] and C.C. YEN[2]
[1]Professor, Departments of Mathematics, Environmental Studies, and Geological Sciences.
California State University, Fullerton, California.
[2]Integral Consultants, Costa Mesa, California.

ABSTRACT

Over the past two decades, the Complex Variable Boundary Element Method (CVBEM) has received increasing attention from engineers and applied mathematicians. The method is used quite often in a variety of engineering and physical science applications. However, until recently and unlike the more commonly used Real Variable Boundary Element Method (RVBEM), the CVBEM could only be applied in a two dimensional geometry. However, current developments have expanded the CVBEM to 3 (or higher) dimensions, eliminating the two-dimensional geometry barrier. In the following pages, we take a brief look at how the 3D CVBEM is applied to a problem with a nonconvex and multiply connected geometry, and draw a conclusion as to how this modern method compares to its real variable counterpart.

2 BACKGROUND FOR THE COMPLEX VARIABLE BOUNDARY ELEMENT METHOD

The Complex Variable Boundary Element Method (CVBEM) is used to develop an approximation function that satisfies the Laplace equation ($\nabla^2 f = 0$) throughout the interior of some problem domain, Ω. The values of the approximation function approach the values of the exact solution of a boundary value problem, for all points on the boundary, by means of a least-squares error minimization.

The problem is set up in a simple form as follows (see Hromadka and Whitley, 1998, and Hromadka & Lai, 1987). Let Ω be a two-dimensional, (2D) simply-connected domain with a simple closed contour boundary, Γ. Let $\varphi(x,y)$ and $\psi(x,y)$ be two-dimensional harmonic functions over $\Omega \cup \Gamma$, that satisfy the Cauchy-Riemann conditions,

$$\frac{\partial \phi}{\partial x} = \frac{\partial \psi}{\partial y}, \frac{\partial \phi}{\partial y} = -\frac{\partial \psi}{\partial x} \tag{1}$$

Being harmonic, they both satisfy the Laplace equation,

$$\frac{\partial^2 \phi}{\partial x^2} + \frac{\partial^2 \phi}{\partial y^2} = 0, \frac{\partial^2 \psi}{\partial x^2} + \frac{\partial^2 \psi}{\partial y^2} = 0. \tag{2}$$

If $z = x + iy$ is a complex variable, then $\varphi(x,y)$ and $\psi(x,y)$ can be written as $\varphi(z)$ and $\psi(z)$. An analytic function $\omega(z)$ is defined over $\Omega \cup \Gamma$ as $\omega(z) = \varphi(z) + i\psi(z)$. The contour boundary, Γ, is subdivided into m boundary elements with nodes specified at each element endpoint (for the

case of a linear trial function on Γ). The boundary elements are given by Γ_j and the endpoints are given by z_j for $j = 1, 2, ...m$. Function values are determined at the nodes using the function values $\omega(z_j)$. A global trial function for $\omega(z)$ is determined for z in Γ by

$$G(z) = \sum_{j=1}^{m} [\omega(z_j) N_j(z) + \omega(z_{j+1}) N_{j+1}(z)], \tag{3}$$

where the N_j are the usual linear basis functions.

Then the CVBEM develops a two-dimensional approximation function $\widehat{\omega}(z)$ of $\omega(z)$ by

$$\widehat{\omega}(z) = \frac{1}{2\pi i} \int_{\Gamma} \frac{G(\zeta)}{\zeta - z} d\zeta . \tag{4}$$

The benefit of using this method comes from the fact that it minimizes the L_2 norm of the difference between $\widehat{\omega}(z)$ and $\omega(z)$ on the boundary of the domain, Γ. Because $\widehat{\omega}(z)$ is analytic, its real and imaginary parts are harmonic in Ω.

2.1 Applying the Problem to Three Dimensions (3D)

Choosing a domain and boundary in three dimensions further complicates the CVBEM problem. Details as the theoretical extension of the CVBEM to three dimensions is given in Hromadka (2001). Also contained in Hromadka (2001) are the application procedures and computer programs to implement the 3D CVBEM. To proceed, we take the subject three-dimensional object and approximate its center of mass. The object is located with a sphere whose radius is slightly larger than the maximum distance from the center of mass to the furthest point on the surface of the object (i.e., an enclosing neighborhood). The enclosing sphere is then translated to the first octant of the 3D space so that all coordinates are positive. The new local coordinate system is denoted by (x^*,y^*,z^*).

We then define a set of projection planes outside of the domain. These projection planes are defined as orthogonal to a set of specified vectors whose originating endpoints are located at the approximated center of mass (i.e., the center of the enclosing sphere). The planes should be distinct and not parallel (see application problem). Finally, the planes are also tangent to the enclosing sphere at the intersection of the corresponding vector with the surface of the sphere.

Next, define a set of integration points on the three-dimensional boundary, Γ. These points are used for the numerical integration process such as used in the usual 2D CVBEM. These integration points are then "projected" on to each of the projection planes. A circle generated by projecting the enclosing sphere onto the plane will surround each of the two-dimensional figures on each of the respective planes. The number of CVBEM nodes for each plane are specified, and these nodes are placed on the circumference of the projected circles. The resulting two-dimensional figures are analyzed using the 2D CVBEM and the local coordinate system, (x^*,y^*,z^*).

Finally we choose a set of test points (other than integration points) on Γ that will be used to determine the accuracy of the method in comparing an available exact solution to the boundary value problems.

2.2 The RVBEM Model

In comparison, the 3D RVBEM used is a linear combination of basis functions of the form $1/R_k$, where R_k is the usual 3D Euclidean distance from RVBEM node k, and the RVBEM approximation, $B(x,y,z)$, is given by

$$B(x,y,z) = \sum_{k=1}^{n} Ck/Rk \tag{5}$$

where n nodes are employed. The C_k are constants determined by a least-squares error minimization fit to the problem boundary conditions, using the same set of problem integration points defined on Γ as used in the 3D CVBEM. Also, the same set of nodes are used for both BEM test trials.

3 TEST PROBLEM DESCRIPTION

Several 3D problems were considered in the current research. The presented application problem is typical of the set of problems considered.

Consider a multiply connected irregular 3D domain which measures 5 units in width, 32 units in length, and 21 units in height (see figure 1). It is noted that the problem boundary, as well as the two interior holes are irregularly shaped and have numerous vertices and cusps.

The approximate center of mass for our shape is estimated at the point (x,y,z) = (3.5, 15.63, 10.77). Notice that there are two holes in our shape, and the diameter for each is set at 2 units. Inside these holes we have source points, P_1 and P_2, located at the centers of the holes and another source point, P_3, located 2.5 units from the right lower corner of our shape. Suppose there is a temperature flow over and inside our domain so that the temperature becomes the potential function we wish to estimate. We are given that the function values at P_1, P_2, and P_3 as 500, 1000 and 500 respectively. The exact solution, which is used for testing the two boundary element methods, is given as

$$F(pj) = \frac{500}{R_1} + \frac{1000}{R_2} + \frac{500}{R_3} \tag{6}$$

where point pj is in Ω, and each

$$R_j = \sqrt{(x_i - x_{p_j})^2 + (y_i - y_{p_j})^2 + (z_i - z_{p_j})^2} \quad , j = 1,2,3. \tag{7}$$

Equations (4) and (5) are used to establish test problem boundary conditions, and also provides the exact solution to compare with numeric results.

Five projection planes with six basis function nodes located on each projection are used for the 3D CVBEM. Thus, a total of 30 CVBEM basis functions are used in the approximation. Each projection plane is determined by defining vectors emanating from the domain's center of mass to a new location which is to be the center of the 2D disk projected onto a plane from the 3D sphere. These displacement vectors are used in such a way that their lengths extend outside the enclosing sphere. The vectors used are (-3.5, 0, 0), (0, -15.63, 0), (0, 0, -10.77), $R\left(\frac{\sqrt{2}}{2}, 0, \frac{\sqrt{2}}{2}\right)$ and $R\left(0, \frac{\sqrt{2}}{2}, \frac{\sqrt{2}}{2}\right)$, where R is the radius of the enclosing sphere. Once these vectors are located, a projection plane perpendicular to these vectors is calculated. The first three planes run parallel to the *XY, XY,* and *YZ* planes. The last two projection planes are at an angle of 45° from the *XZ* plane (see figures 2 & 3).

Each projection results in an image of a circle with 6 CVBEM nodes evenly spaced along the perimeter. When using the CVBEM program, the position of the nodes is automatically computed and used to compute an approximation for the exact solution. These nodal locations are also used for the RVBEM of (5).

4 RESULTS AND CONCLUSIONS

The information below details the results from applying the two methods to the test problem.

Table 1: 3D CVBEM Results

STATISTICS ON TEST POINT SET:
NUMBER OF TEST POINTS = 831
SUM OF SQUARED RESIDUAL = .2364D+07
MAXIMUM VALUE OF APPROXIMATION = .4967E+03
MINIMUM VALUE OF APPROXIMATION = .9288E+02

MAXIMUM ABSOLUTE DIFFERENCE = .5364D+03
AT LOCATION: TEST POINT #412; EXACT = .9401D+03; APPROX. = .4037D+03; MAX ERROR = .5364D+03; RE = .5906D+00
MAXIMUM RELATIVE ERROR = .5706D+00; AVERAGE RELATIVE ERROR = -.1199D-□01
AT LOCATION: TEST POINT #412; EXACT = .9401D+03; APPROX. = .4037D+03; ERROR = .5364D+03; MAX RE = .5706D+00

Table 2: 3D RVBEM Results

STATISTICS ON TEST POINT SET:
NUMBER OF TEST POINTS = 831
SUM OF SQUARED RESIDUAL = .2993D+07
MAXIMUM VALUE OF APPROXIMATION = .4557E+03
MINIMUM VALUE OF APPROXIMATION = .1110E+03

MAXIMUM ABSOLUTE DIFFERENCE = .5637D+03
AT LOCATION: TEST POINT #412; EXACT = .9401D+03; APPROX. = .3764D+03; MAX ERROR = .5637D+03; RE = .5996D+00
MAXIMUM RELATIVE ERROR = .5996D+00; AVERAGE RELATIVE ERROR = -.1678D-01
AT LOCATION: TEST POINT #412; EXACT = .9401D+03; APPROX. = .3764D+03; ERROR = .5637D+03;
MAX RE = .5996D+00

Examining the sum of square residuals and the average relative error, we conclude that the CVBEM produces the smaller error. The average relative error for the CVBEM is about 1.2% of the true value of our potential function. In comparison, the RVBEM produces an average relative error of about 1.7%. Consequently, it would seem that the CVBEM is the better method for estimating the actual potential function for our problem. Although the CVBEM seems to be superior over the RVBEM, observing the maximum absolute difference between two methods gives us added insight in comparing the two methods. The CVBEM shows this value to be 536.4 while the RVBEM show the same statistic as 563.7.

In the accompanying figures, we compare exact and approximate solutions in addition to absolute and relative errors at our test points. Focus is paid on both sides of the 3D object ($x = 1$; $x = 6$), and also on a slice through the center of the object ($x = 3.5$). The figures provide an added insight as to where upon the object the two methods fared best and serve to identify areas requiring further investigation into how to reduce these errors.

5 REFERENCES

1. Hromadka II, Theodore V., Whitley, Robert J. Advances in the Complex Variable Boundary Element Method, Springer-Verlag New York, 1998.
2. Hromadka II, Theodore V., Lai, Chintu, The Complex Variable Boundary Element Method in Engineering Analysis, Springer-Verlag New York, 1987.
3. Hromadka II, T.V., Dissertation, A Multi-Dimensional Complex Variable Boundary Element Method, Wessex Institute of Technology, University of Wales, Swansea, April 2001.

6 LIST OF FIGURES

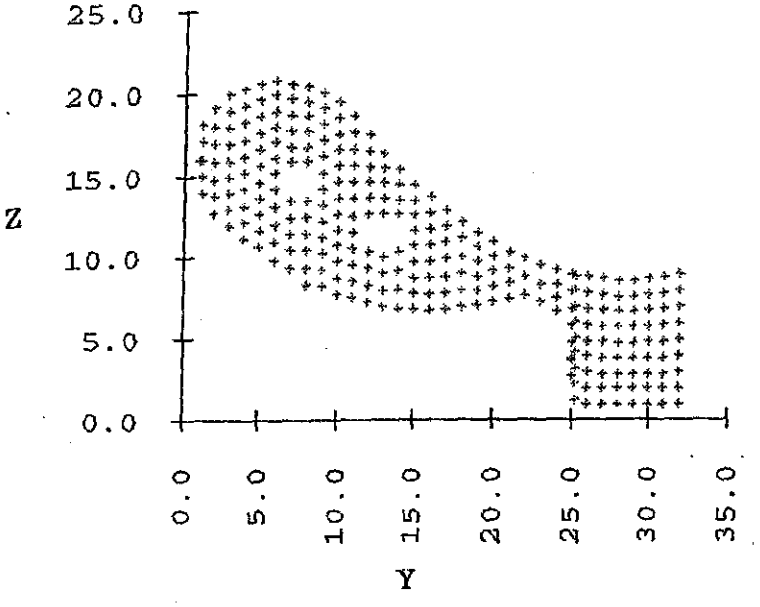

Figure 1: 3-D Object (Uniform Thickness) in Original Y-Z Plane, showing integration point coverage on problem boundary. Note two holes in the problem domain.

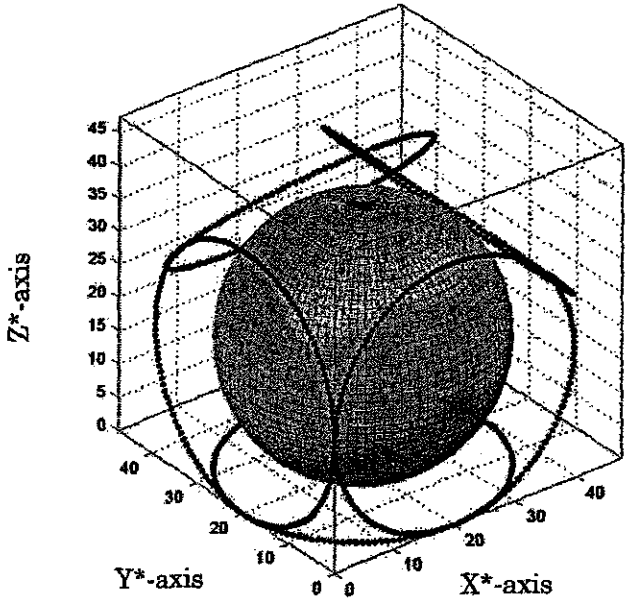

Figure 2: Example problem enclosing sphere with resulting circles from projecting sphere onto 5 projection planes

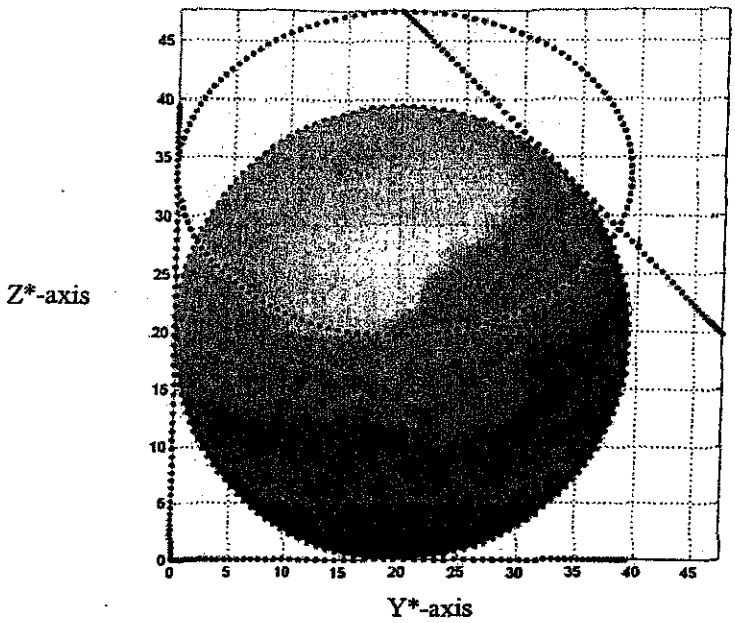

Figure 3: Y-Z axis View of Figure 2. Note resulting 5 circle projections.

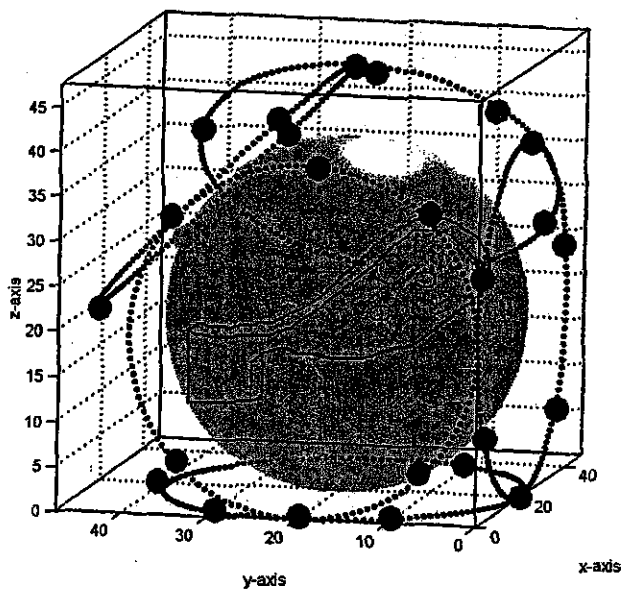

Figure 4: Problem Domain within Enclosing Sphere with CVBEM (or RVBEM) Basis Nodes projected onto the 5 Projection Planes. Basis nodes (total of 30) are shown as the large dots on the projected circles.

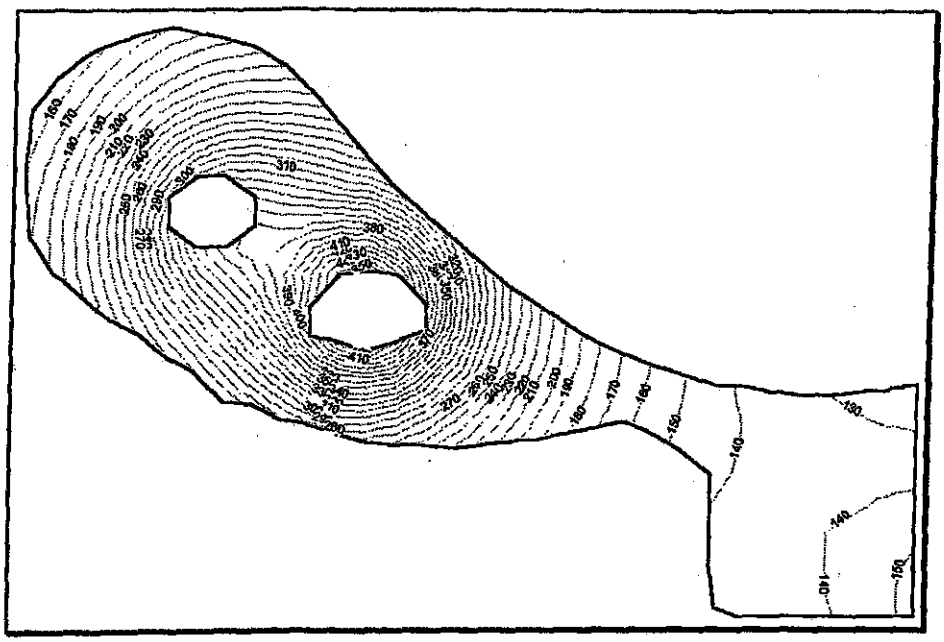

Figure 5: Exact Solution Plot at $X = 1$ (local coordinate X* = 17.17).
Note irregular boundary containing numerous vertices.

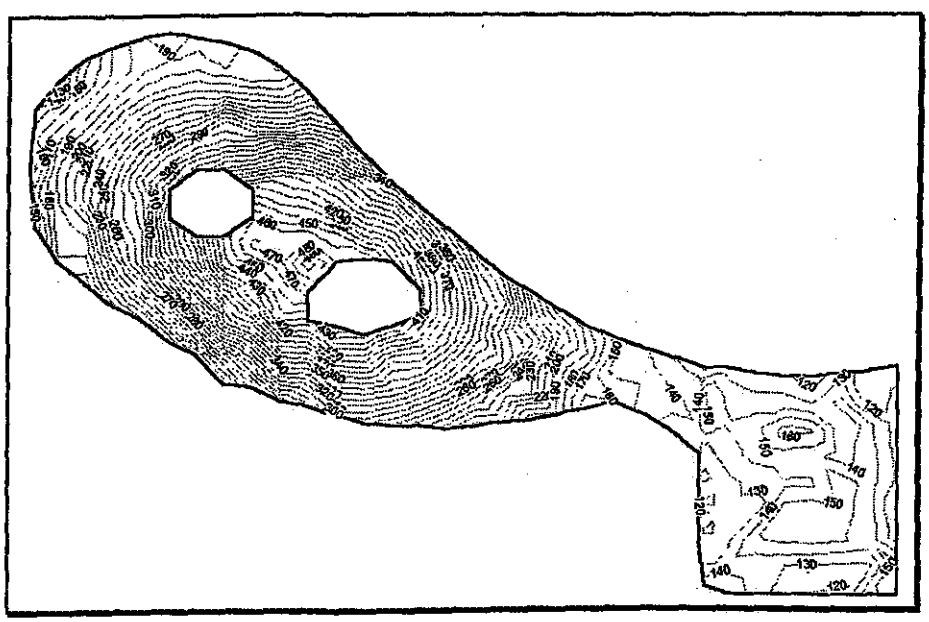

Figure 6: CVBEM Approximations at $X = 1$ (local coordinate X* = 17.17).

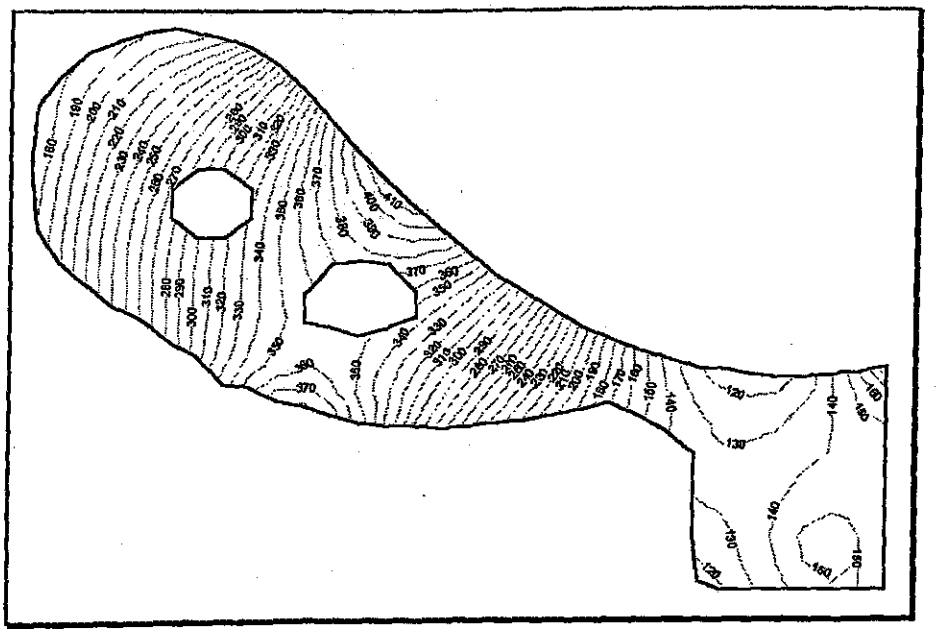

Figure 7: RVBEM Approximations at $X = 1$ (local coordinate X* = 17.17).

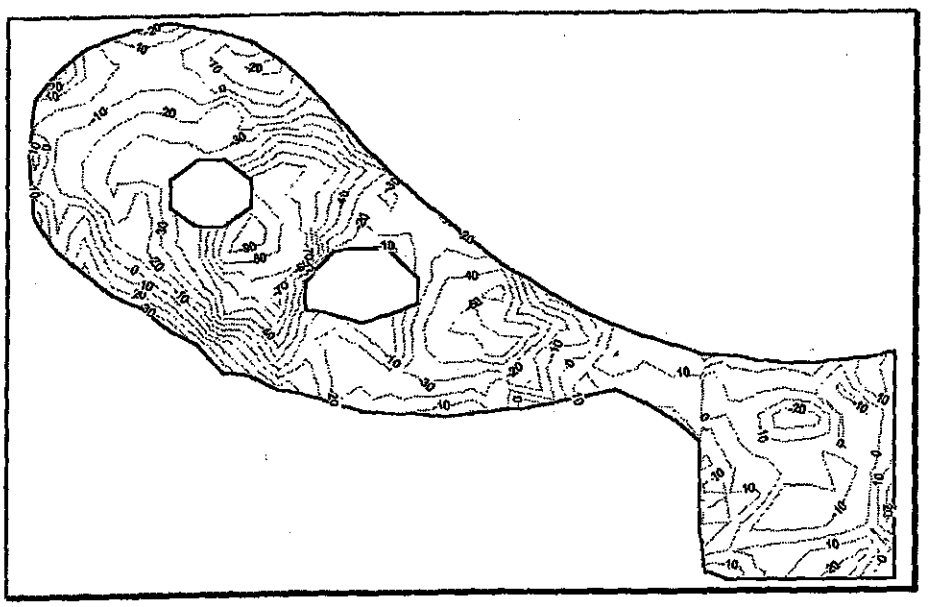

Figure 8: CVBEM Approximation Error at $X = 1$ (local coordinate X* = 17.17).

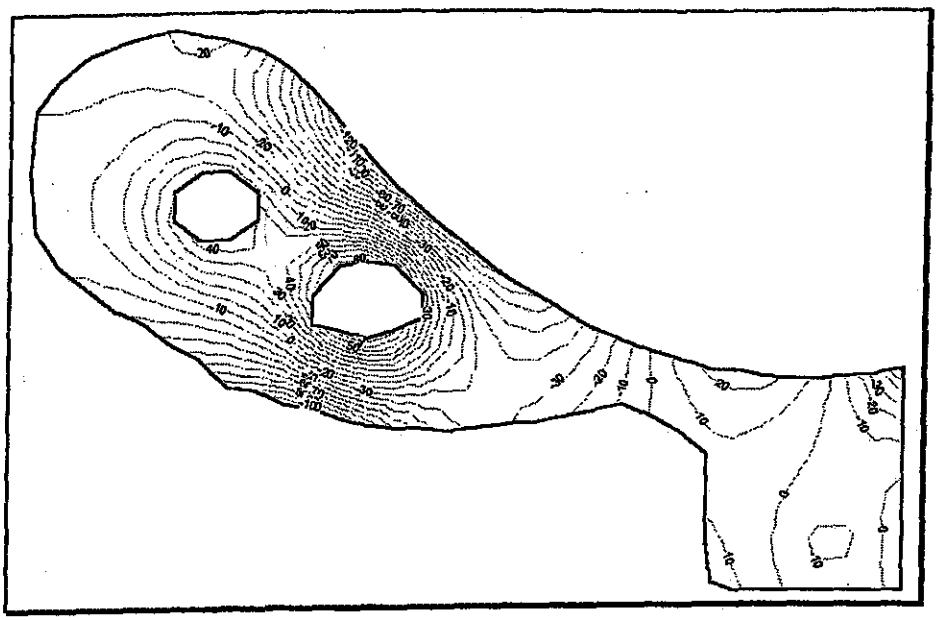

Figure 9: RVBEM Approximation Error at $X = 1$ (local coordinate X* = 17.17).

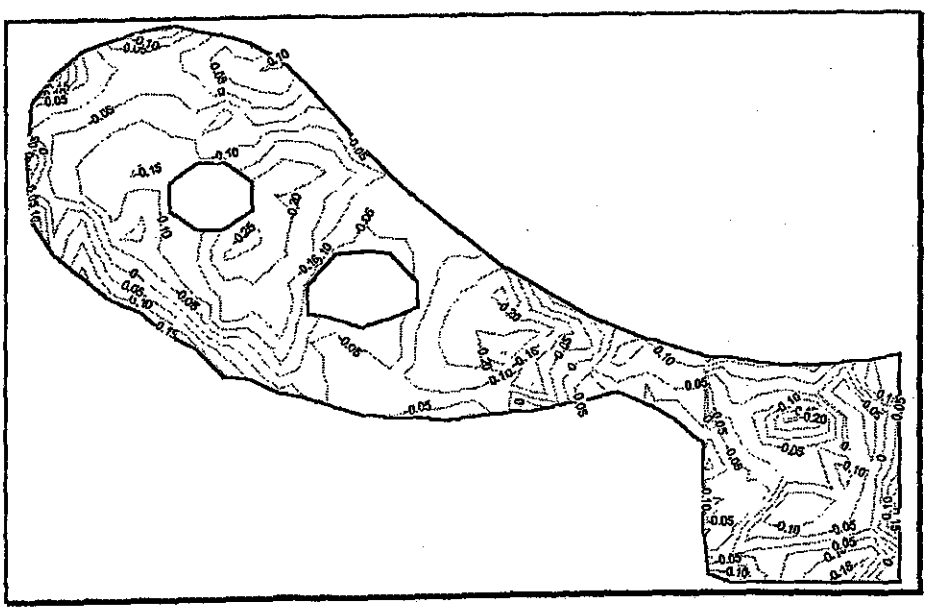

Figure 10: CVBEM Relative Errors (decimal) at $X = 1$ (local coordinate X* = 17.17).

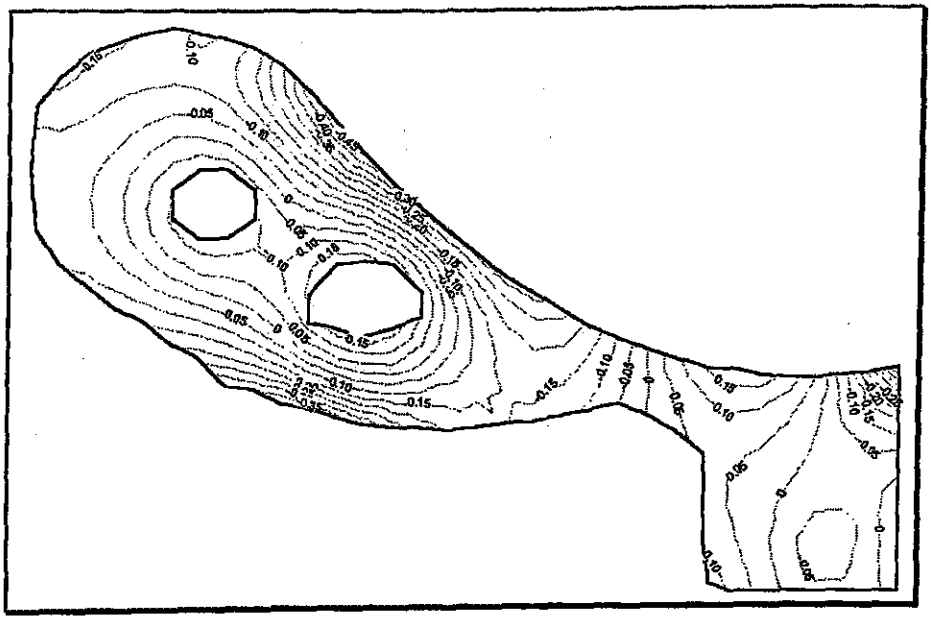

Figure 11: RVBEM Relative Errors (decimal) at $X = 1$ (local coordinate X* = 17.17).

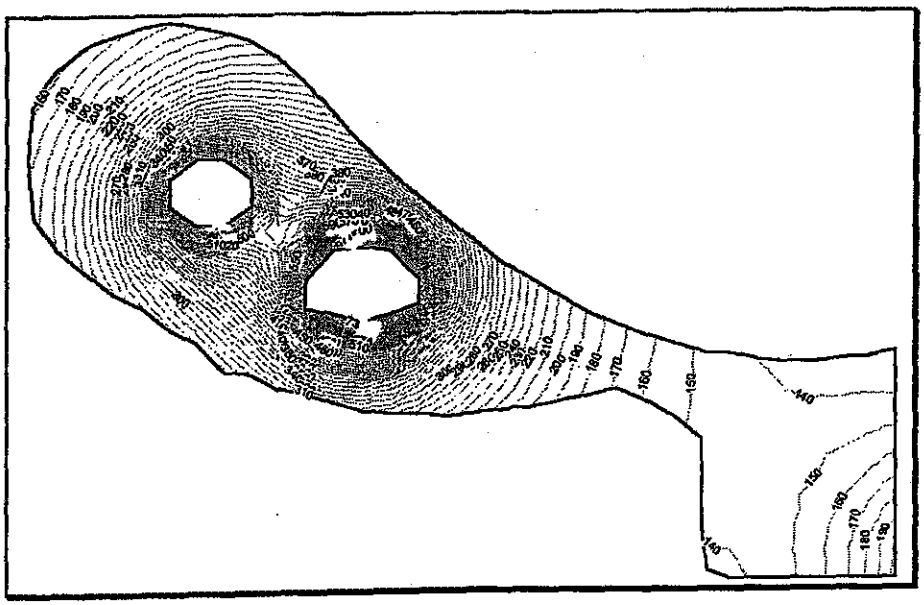

Figure 12: Exact Solution Plot at Slice through center of Ω, $X = 3.5$ (local coordinate X* = 19.67).

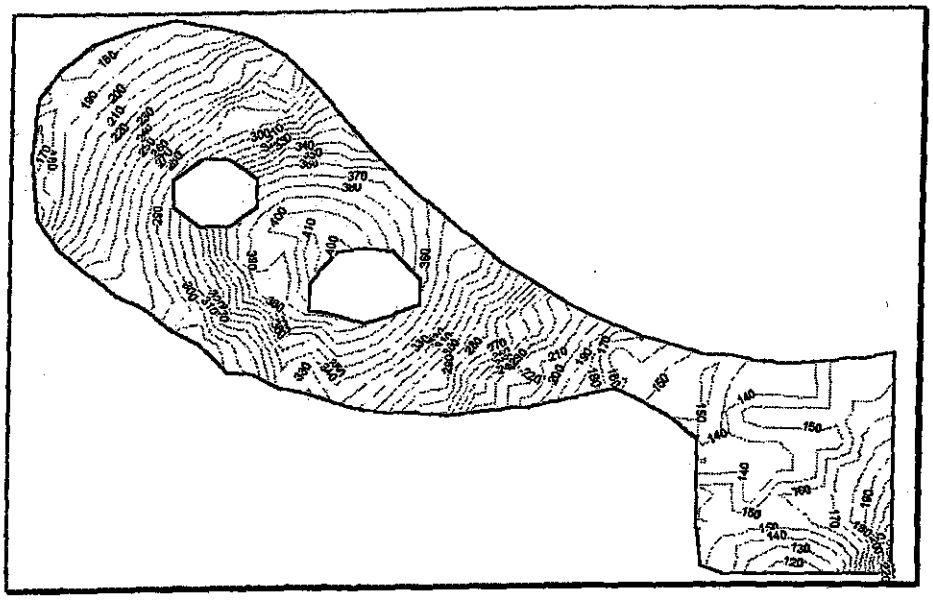

Figure 13: CVBEM Approximations at $X = 3.5$ (local coordinate X* = 19.67).

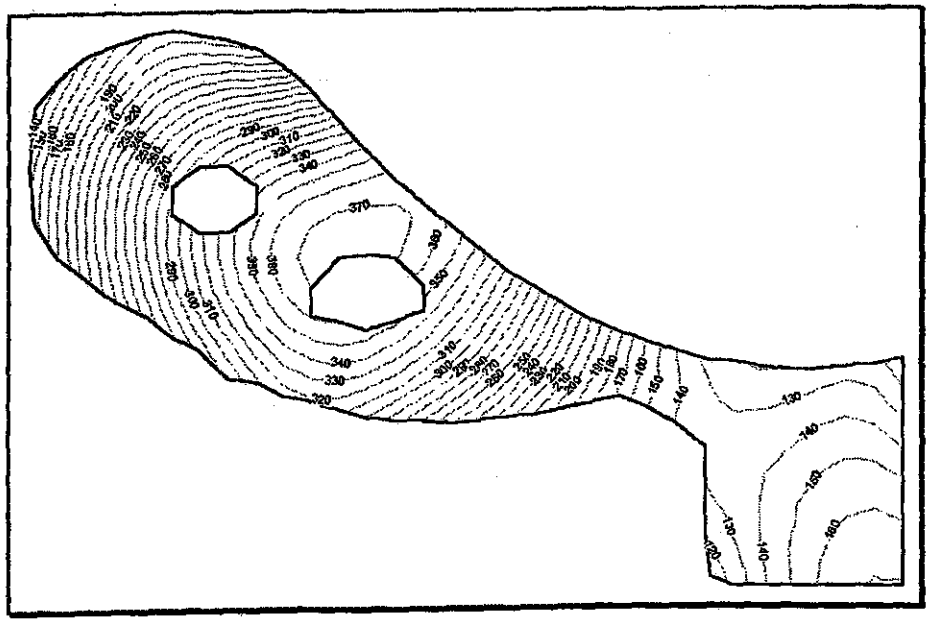

Figure 14: RVBEM Approximations at $X = 3.5$ (local coordinate X* = 19.67).

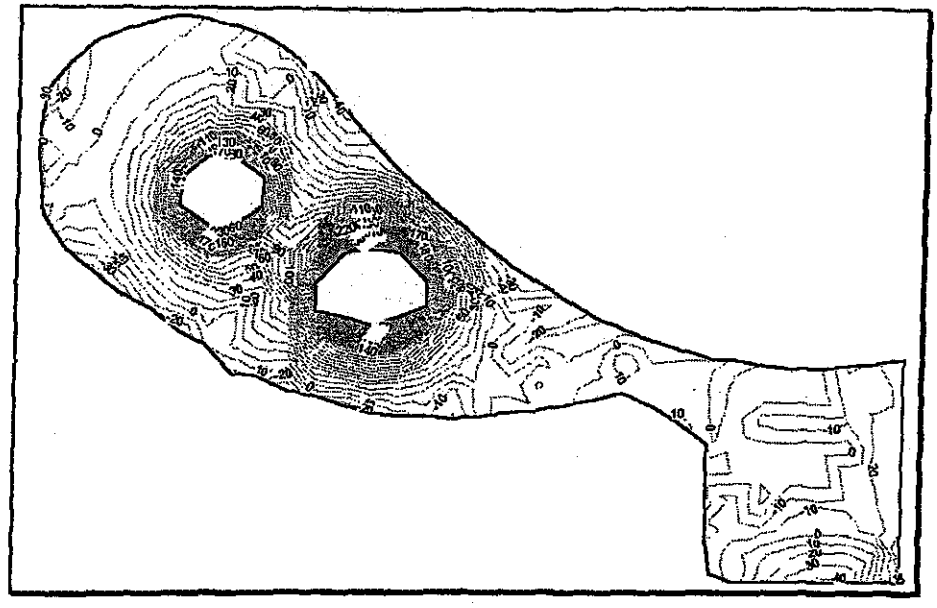

Figure 15: CVBEM Approximation Error at $X = 3.5$ (local coordinate X* = 19.67).

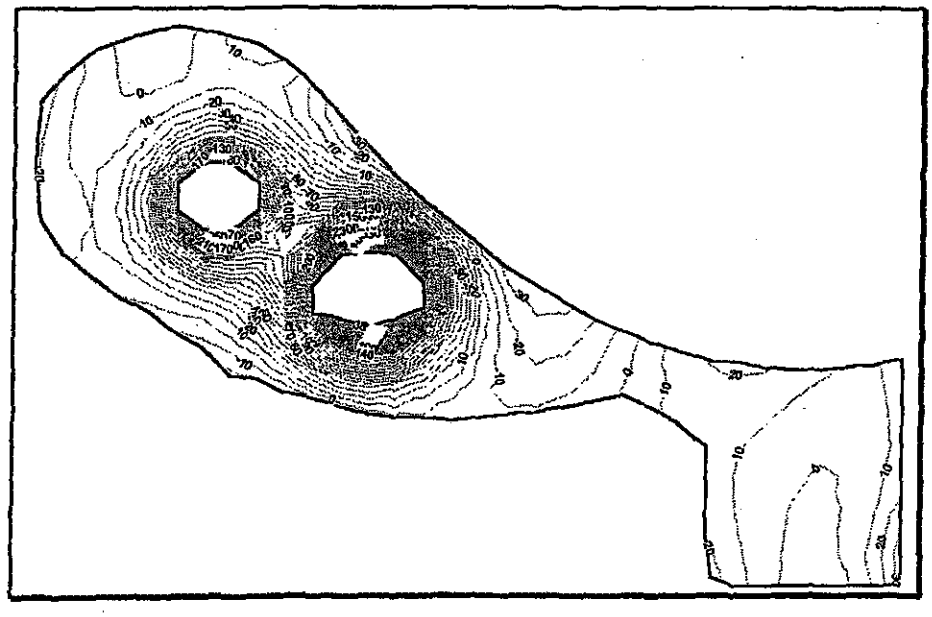

Figure 16: RVBEM Approximation Error at $X = 3.5$ (local coordinate X* = 19.67).

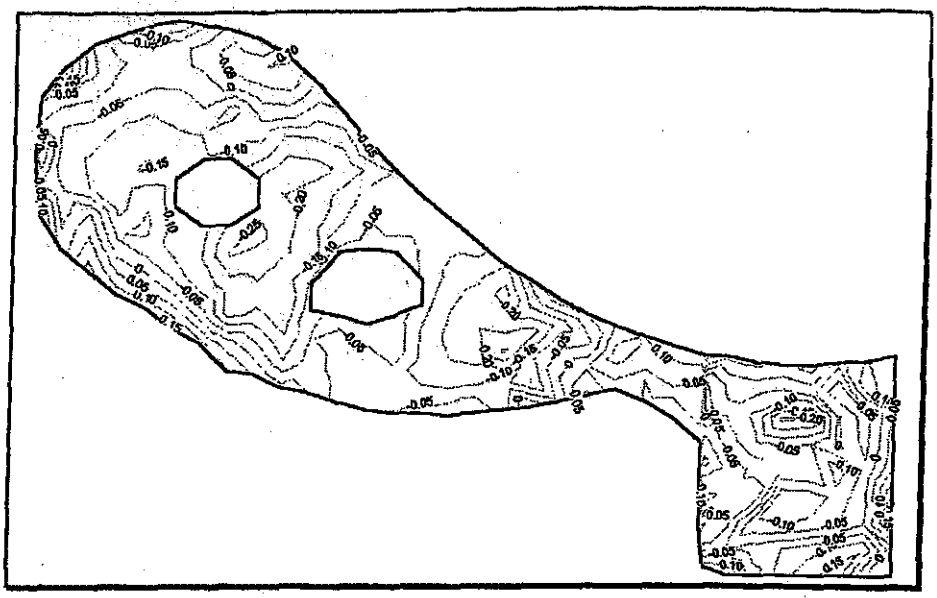

Figure 17: CVBEM Relative Errors (decimal) at $X = 3.5$ (local coordinate X* = 19.67).

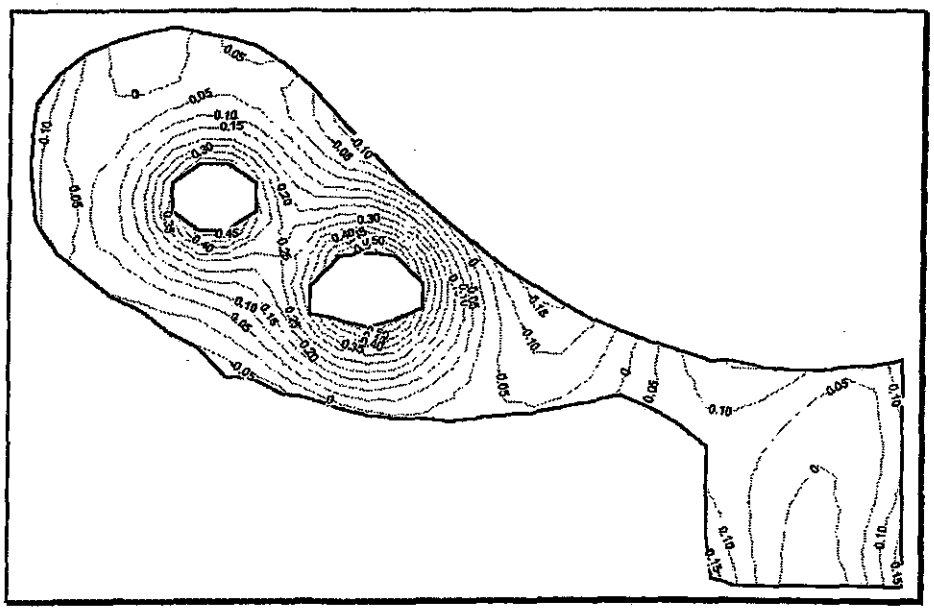

Figure 18: RVBEM Relative Errors (decimal) at $X = 3.5$ (local coordinate X* = 19.67).

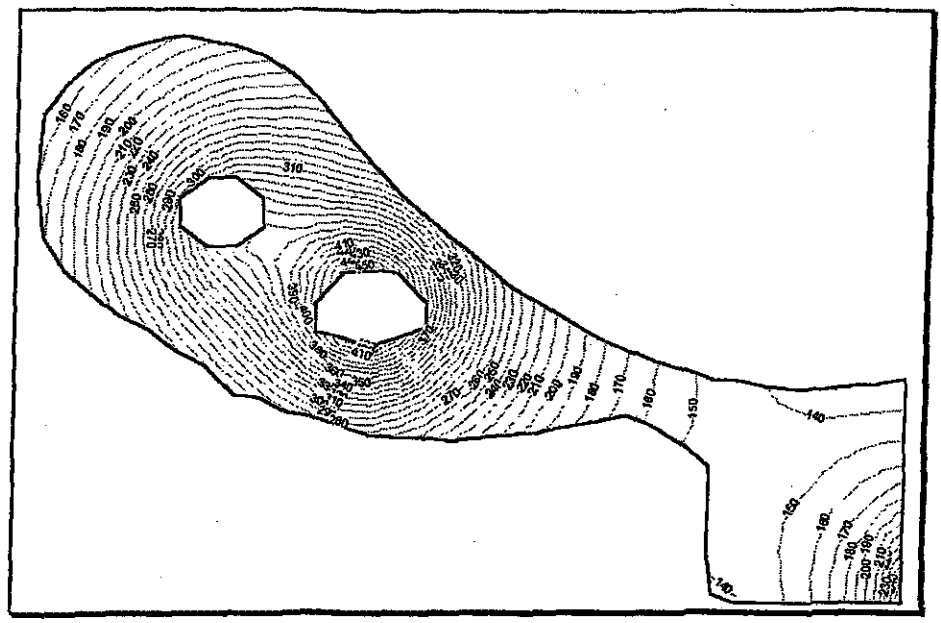

Figure 19: Exact Solution Plot at X = 6 (local coordinate X* = 22.17).

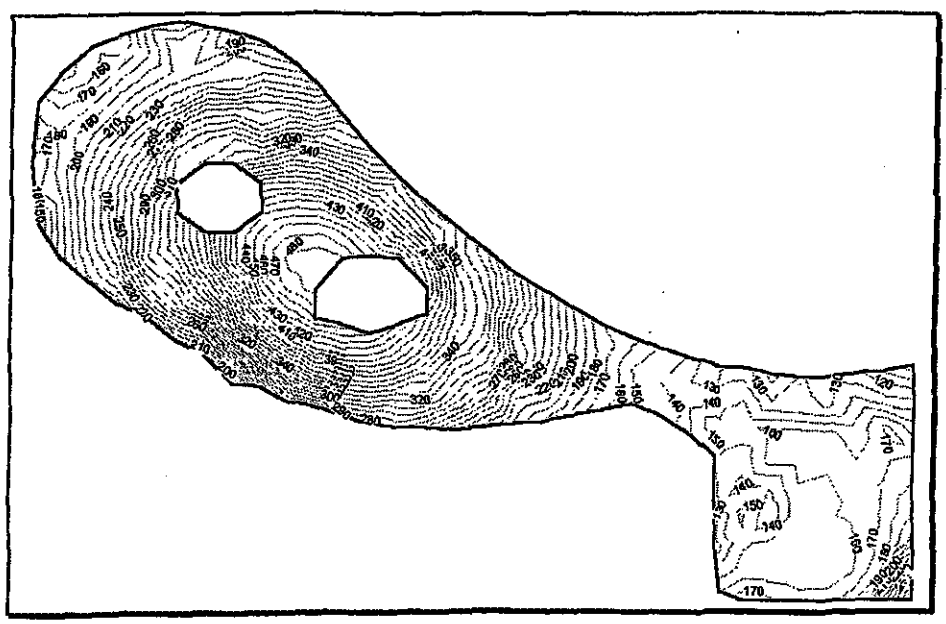

Figure 20: CVBEM Approximations at $X = 6$ (local coordinate X* = 22.17).

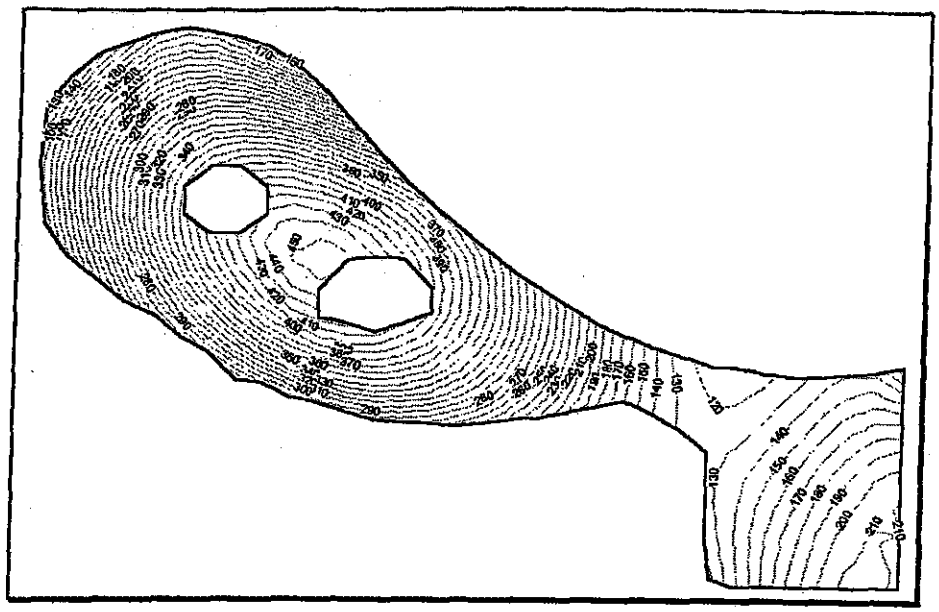

Figure 21: RVBEM Approximations at X = 6 (local coordinate X* = 22.17).

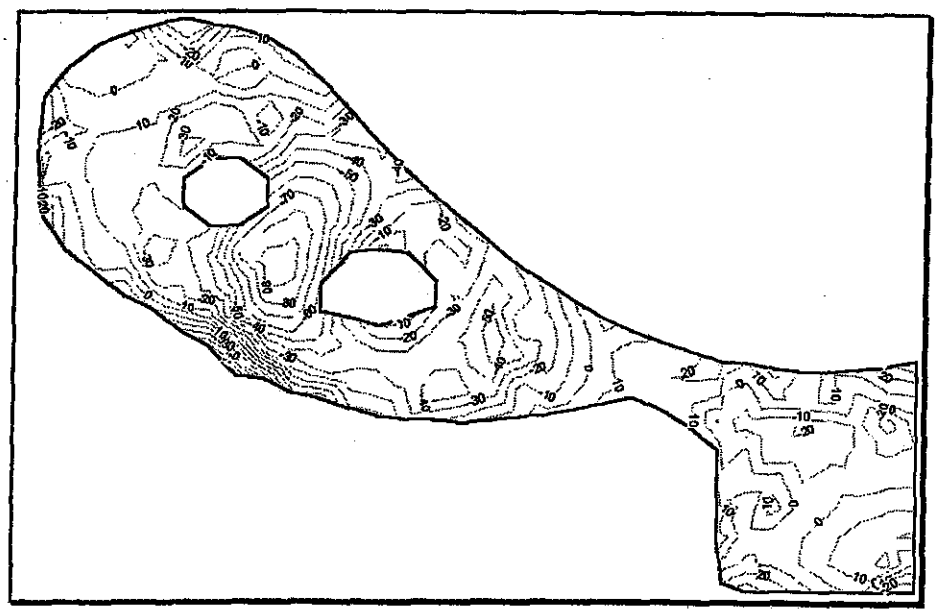

Figure 22: CVBEM Approximation Error at $X = 6$ (local coordinate X* = 22.17).

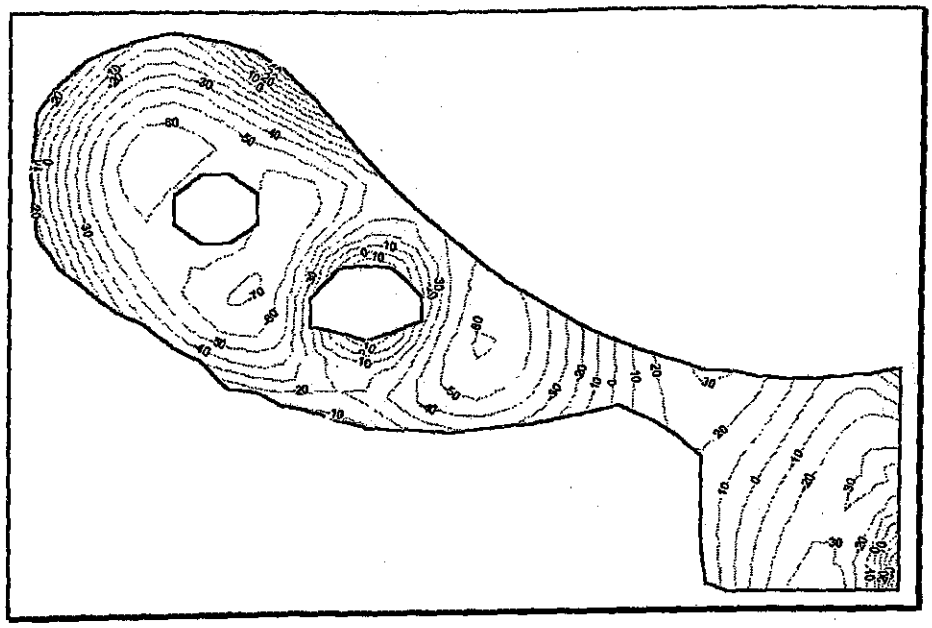

Figure 23: RVBEM Approximation Error at $X = 6$ (local coordinate X* = 22.17).

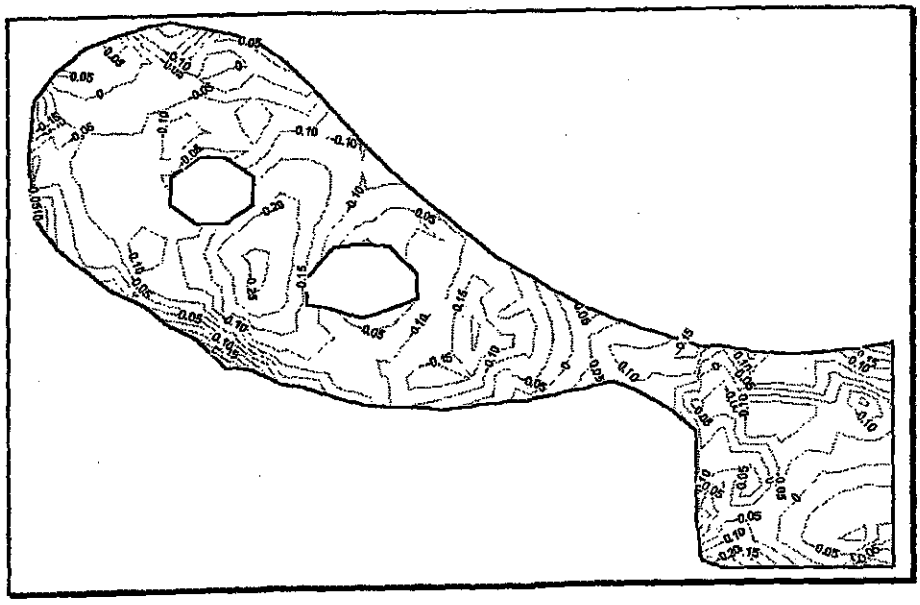

Figure 24: CVBEM Relative Errors (decimal) at $X = 6$ (local coordinate X* = 22.17).

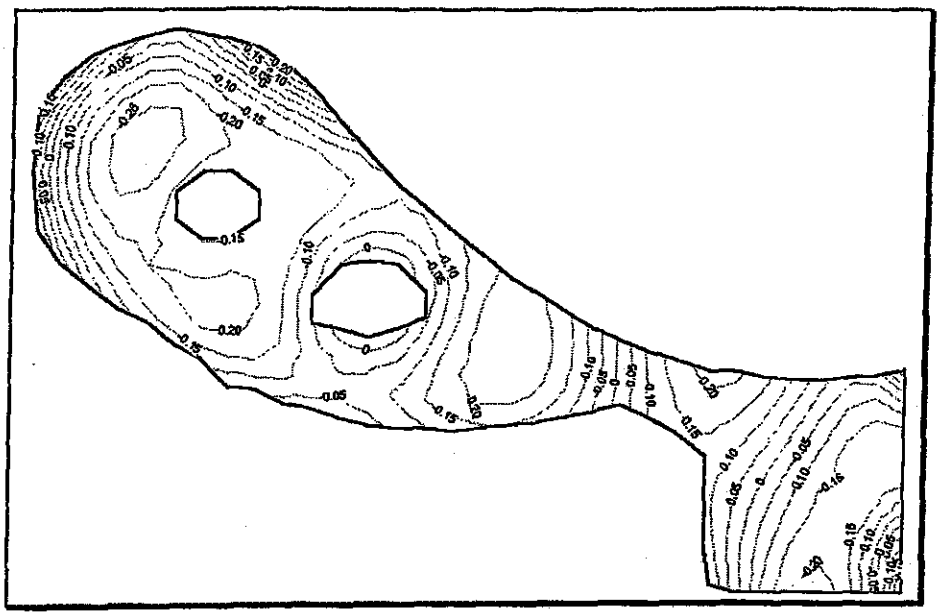

Figure 25: RVBEM Relative Errors (decimal) at $X = 6$ (local coordinate X* = 22.17).